Article ID: 1000-7032(2022)06-0851-11

Fabrication and Spectroscopic Properties of Heavily Pr^{3+} Doped Selenide Chalcogenide Glass and Fiber for Mid-infrared Fiber Laser

XU Chen-yu[1,2], CUI Jian[1,2], XU Yan-tao[1], XIAO Xu-sheng[1], CUI Xiao-xia[1], GUO Hai-tao[1,2*]

(1. *State Key Laboratory of Transient Optics and Photonics, Xi'an Institute of Optics and Precision Mechanics, Chinese Academy of Sciences, Xi'an* 710119, *China*;
2. *University of Chinese Academy of Sciences, Beijing* 100049, *China*)
* *Corresponding Author, E-mail: guoht_001@opt. ac. cn*

Abstract: In order to develop a high gain medium for fiber lasers operating at 3-5 μm waveband, 0-0.4% (in weight) Pr^{3+} ions doped $Ge_{12}As_{20.8}Ga_4Se_{63.2}$ selenide chalcogenide glasses were prepared and the 0.2% (in weight) Pr^{3+} ions doped one was successfully drawn into step-index double-cladding fiber with the lowest loss of 2.95 dB/m@6.58 μm by a multistage rod-in-tube method. The electron-probe measure microanalysis (EPMA), X-ray diffraction (XRD), differential scanning calorimeter (DSC), field emission transmission electron microscope (FE-TEM), transmission and mid-infrared fluorescence spectra were carried out to analyze the dispersion of Pr^{3+} ions in glass, the impurity contents, thermal and optical changes caused by the Pr^{3+} ions' introduction. By analyzing the absorption and emission measurements of the serial glasses with the Judd-Ofelt theory, the Judd-Ofelt strength parameters, transition probabilities, exited state lifetime, branching ratios, and emission cross-sections were also calculated. This selenide chalcogenide glass has high Pr^{3+} ions' solubility and emission characteristic, good thermal stability and fiber forming performance, indicating that it has potential to be used as mid-infrared laser working medium.

Key words: chalcogenide glass; rare-earth ions; spectroscopy; mid-infrared fluorescence; infrared fiber
CLC number: O482.31 **Document code**: A **DOI**: 10.37188/CJL.20220088

用于中红外光纤激光器的高 Pr^{3+} 掺杂硒化物硫系玻璃和光纤制备及其光谱特性

许晨煜[1,2], 崔 健[1,2], 许彦涛[1], 肖旭升[1], 崔晓霞[1], 郭海涛[1,2*]

(1. 中国科学院西安光学精密机械研究所 瞬态光学与光子技术国家重点实验室, 陕西 西安 710119;
2. 中国科学院大学, 北京 100049)

摘要: 为了研发用于3~5 μm波段光纤激光器的增益介质,制备了重量百分比为0~0.4%不同浓度 Pr^{3+} 离子掺杂的 $Ge_{12}As_{20.8}Ga_4Se_{63.2}$ 硒化物硫系玻璃。通过多级棒管法,重量百分比为0.2%的 Pr^{3+} 离子掺杂玻璃被成功拉制成阶跃型双包层光纤,损耗最低为2.95 dB/m(位于6.58 μm处)。采用电子探针显微分析(EPMA)、X射线衍射(XRD)、差示扫描量热(DSC)、场发射透射电子显微镜(FE-TEM)、透射光谱和中红外荧光光谱分析了玻璃中

收稿日期: 2022-03-15; **修订日期**: 2022-03-27
基金项目: 国家自然科学基金(62005312, 62090065, 61935006); 中国科学院创新交叉团队项目(JCTD-2018-19)资助
Supported by National Natural Science Foundation of China (62005312, 62090065, 61935006); Chinese Academy of Sciences Interdisciplinary Innovation Team Project (JCTD-2018-19)

Pr^{3+}离子的分散性、杂质含量以及Pr^{3+}离子引入引起的热、光学性质变化。通过玻璃的吸收和发射光谱并结合Judd-Ofelt理论，计算了Judd-Ofelt强度参数、辐射跃迁几率、荧光寿命、荧光分支比和受激发射截面。这种硒化硫系玻璃具有较高的Pr^{3+}离子溶解度和中红外发光特性、良好的热稳定性和成纤性能，表明其具有作为中红外激光工作介质的潜力。

关 键 词：硫系玻璃；稀土离子；光谱学；中红外荧光；红外光纤

1 Introduction

Rare-earth(RE) ions doped fiber lasers operating at mid-infrared(MIR) regions are of great interests due to their potential applications in fields of chemical sensing, air pollution monitoring, medical surgery, national defense, and *etc*[1-4]. Chalcogenide glasses (ChGs), as hosts for RE ions, have their unique advantages. The ChGs' phonon energies are as low as 250-425 cm^{-1}, especially in which the selenide glasses have lower phonon energies of 250-300 cm^{-1}[5]. This results in lower probabilities of multi-phonon transitions for RE ions, making it easier to achieve higher efficient MIR transitions of RE ions.

It is known that the RE ions doped fluoride fibers have achieved high-power laser output in 3 μm waveband[6-7], and compared with fluoride ones, ChG fibers have no obvious advantage for laser output at below 4 μm. Because of this, in the past two decades, people paid much attention to realize laser output at ≥4 μm wavelength in ChG fibers[8-11]. However, there has been little experimental progress in the research of ChGs' fibers in laser output. There are three main reasons including the low RE ions' solubility, the still high multi-phonon relaxation rate of RE ions and the severe fiber loss originating from impurities' absorption[12-13].

Recently, a longest laser output wavelength as well as 5.14 μm was reported in a 0.05% (in weight, the same below) Ce^{3+}-doped $Ge_{15}As_{21}Ga_1Se_{63}$ fiber with a 9 μm-core-diameter pumped by a 4.15 μm quantum cascade laser at room temperature[14]. Ge-As-Ga-Se (GAGSE) glass system is interested because of its two advantages. Firstly, compared with the stubborn S—H bonds in sulfide glasses, Se—H bonds are easier to be eliminated because of lower polarity and bond energy(339 kJ/mol for S—H and 314 kJ/mol for Se—H). Secondly, the conventional As—Se system glasses have strong covalence, resulting in the tendency of clustering of RE ions and quenching of fluorescence. Based on the original glass network, the introduction of Ge can improve the compactness of glass grid and increase the laser damage threshold[15-16], which means the glass can be pumped by a higher power laser. However, there are a large number of Se—Se bridging bonds and Ge—Se covalent bonds in Ge—As—Se, which cannot compensate the high coordination number of RE ions, resulting in the low RE's solubility. Ga is further introduced to compensate for negative local environment of positive RE ions by forming Ga—Se—RE^{3+} [9]. Introduction of Ga is effective to weaken the aggregation of RE ions in glass matrix.

Several researchers have conducted many studies of RE ions doped GAGSE glasses and fibers. In 2014, Tang *et al*. prepared a 0.05% Pr^{3+} ions doped GAGSE fiber by the extrusion method, and the lowest loss of fiber is 2.8 dB/m at 6.65 μm[8]. In 2018, Liu *et al*. prepared the Pr^{3+} ions doped $Ge_{10}As_{24}Ga_4Se_{62}$ glass and fiber with an optimal doping concentration of 0.2%. The 250/125 μm(cladding diameter/core diameter), 0.2% doped step-index fiber exhibited the lowest loss of 3.5 dB/m at 6.9 μm. The fiber loss is about 10 dB/m at 2.9 μm caused by O—H bonds and 7 dB/m at 6.3 μm caused by H_2O molecule[9]. In order to remove impurities and achieve low-loss GAGSE fibers, Shiryaev *et al*. reported a special chemical reaction device to transfer the GaI_3 vapor stream into the reactor for preparation of $Ge_{16}As_{17}Ga_3Se_{64}$ glasses[17]. This provides a practical idea for the preparation and purification of Ga-containing GAGSE glasses. In 2018, they successfully fabricated a low-loss $Ge_{25}As_{15}Ga_3Se_{57}$ single-index fiber by using metallic aluminum and $TeCl_4$ for purification.

The minimum fiber loss is 0.6 dB/m at 6.7 μm and the optical loss is about 5 dB/m at 4.58 μm caused by Se—H bonds[18]. However, there are still few reports about fiber laser output of Pr^{3+} ions. This is mainly because the severe absorption of impurities and weak fluorescence intensity in Pr^{3+} doped ChG fibers. So far, the doping concentration of Pr^{3+} ions in ChG fibers reported is relatively low (usually 0.5%). Therefore, the successful fabrication of a heavily Pr^{3+} doped CHG fiber with low impurity absorption has become an urgent requirement.

In this work, a modified glass composition of $Ge_{12}As_{20.8}Ga_4Se_{63.2}$ was designed and a serial glasses doped with different concentration of Pr^{3+} ions were prepared. This composition glass has higher Pr^{3+} ions solubility (at least 0.4% without crystallization), and the 0.2% Pr^{3+}-doped glass was drawn into fiber with double-cladding structure. For reducing content of impurities (oxygen, hydrogen, carbon, silicon, and *etc.*), the raw materials were distilled and the glasses were introduced with chemical impurity removal reagent. The absorption and emission spectra of bulk glasses were investigated and Judd-Ofelt intensity parameters were calculated. Broadband MIR luminescence of Pr^{3+} ions in the region of 3.3–5.5 μm was observed, and the stimulated emission cross-section, radiation lifetime and other parameters were calculated.

2 Experiment

2.1 Glass Preparation and Fiber Drawing

$Ge_{12}As_{20.8}Ga_4Se_{63.2}$ glass samples doped with 0, 0.05%, 0.1%, 0.2%, 0.3% and 0.4% in weight of Pr^{3+} ions (denoted as GAGSE-undoped, GAGSE-0.05, GAGSE-0.1, GAGSE-0.2, GAGSE-0.3 and GAGSE-0.4) were prepared by melt quenching method. The raw materials of Ge (6N, grains, Nanjing Germanium Co., Ltd., RRC), Ga (7N, grains, Aladdin Industrial Co. Ltd., RRC) and Praseodymium powder (3N, powder, Aladdin Industrial Co. Ltd., RRC) were respectively packed in ampoules and heated to remove volatile impurities. The As (7N, grains, Mount Emei Jiamei High Pure Material Co. Ltd., R. R. C.) and Se (6N, Aladdin Industrial Co. Ltd., RRC) were purified by a multi-stage distillation progress. All of the raw materials were weighed by an analytical balance (Sartorius, resolution of 0.001 g) in the glovebox (N_2-filled, $O_2 \leqslant 10^{-8}$, $H_2O \leqslant 10^{-8}$), then loaded Ge, As, Se into a pre-treated quartz ampoule (800 ℃ for 12 h, under vacuum of 10^{-3} Pa). The ampoule was sealed under vacuum (10^{-3} Pa), and initially melted at 900 ℃ for 10 h to homogenize host glasses. The initial melted sample was transferred to a customized distillation ampoule, and Al foil (5N, Aladdin Industrial Co. Ltd., RRC) was introduced as deoxidizer. The distilled compound was then mixed with Ga and Pr powder and melted at 850 ℃ for 8 h. Subsequently, the quartz ampoule containing the molten glass was quenched, annealed near the glass transition temperature, and slowly cooled to the room temperature. The samples were cut into disks with a diameter of 12 mm and thickness of 3 mm, and mirror polished of both sides for following measurements.

The glass sample which has the best optical and thermal properties was selected to be drawn into fiber by a multistage rod-in-tube method (see Fig. 1). In order to achieve single-mode transmission and control the diameter of fiber easily during the fiber drawing, a double-cladding structure was designed. The cladding tubes were prepared by the rotational casting method. After the core rod and inner-cladding tube were combined, they were predrawn into a slim rod (external diameter d=2.6 mm). Then we assembled this preform with a thick outer-cladding tube which has a small hole through the center (internal diameter d'=3.0 mm), then coated it with FEP tube (external diameter d=15.0 mm). Finally, the single-mode, double-cladding fiber with a diameter of 125 μm was drawn from the assembly. The optical fiber draw tower (SG Control, UK; MT-600N) is equipped with a built-in furnace which heated the preform to 440 ℃ at a heating rate of 2 ℃/min and kept this temperature to draw the optical fiber. During the drawing process, the He was introduced for atmosphere protection.

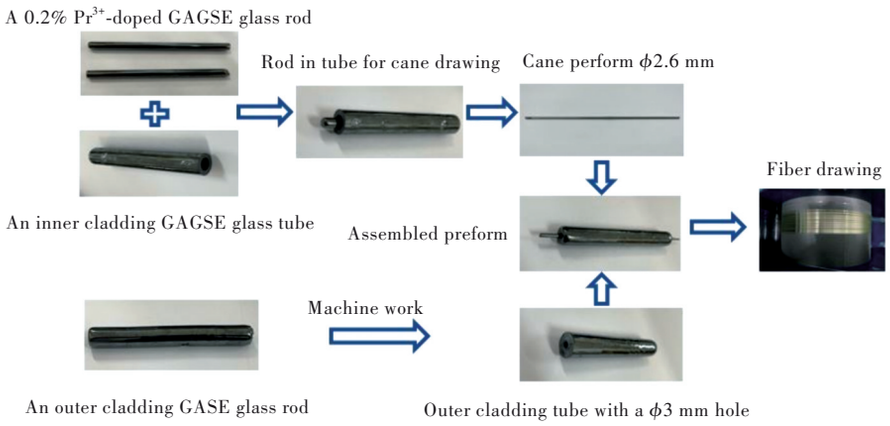

Fig. 1 The fabrication process of 0.2% Pr^{3+}-doped, single-mode and double-cladding $Ge_{12}As_{20.8}Ga_4Se_{63.2}$ glass fiber.

2.2 Physical and Optical Measurements

To figure out the composition deviation of the glass samples caused by the chemical purification treatment, the electron-probe measure microanalysis (EPMA, JEOLJXA-8230) was carried out. All samples were analyzed for the presence of crystalline phases by X-ray diffraction (XRD) (Bruker D8 ADVANCE with Cu radiation, a power of 40 kV, 40 mA, a step size of 0.02°(2θ) and step time of 0.1 s). The thermal characteristics of the samples were analyzed by a Differential Scanning Calorimeter (NETZSCH DSC 404 F3). 15 mg of glass powder was put into an aluminum crucible and heated to 400 ℃ under the protection of flowing atmosphere(N_2) with a heating rate of 10 ℃/min. The Field Emission Transmission Electron Microscope (FE-TEM) (FEI-Talos F200S/FEI Tecnai G2 F20 X-Twin) was used to verify the amorphous properties of the glass and the dispersion of RE ions with an Energy Dispersive Spectrometer (EDS). The accelerating voltage regulation range is 20–200 kV and the maximum magnification can exceed 1 000 000 times. The point resolution and line resolution can reach 0.24 nm and 0.102 nm, respectively. The glass samples for FE-TEM are ground into fine powder, and then dispersed in absolute ethanol. The density measurement of the samples is Archimedes method, using a high-precision balance with special accessories. UV-VIS-NIR transmission spectrum of glass was measured by a spectrophotometer (JASCO V-570). The region was 400–2 500 nm and the step length was 2 nm. FT-IR spectroscopy was measured by BRUKER VERTEX 70 and the region was 2–23 μm. The MIR fluorescence spectrum was measured by a fluorescence spectrometer (FSP920; Edinburgh Instruments Ltd., UK) equipped with a liquid-nitrogen cooled InSb detector (C4159-5671; HAMAMATSU, JPN). The measurement wavelength was 2 300–5 500 nm and the spectral step size was 2 nm, pumped by a 2 μm CW laser.

3 Results and Discussion

3.1 Amorphous and Thermal Properties

Tab. 1 is the EPMA analytical compositions of the undoped GAGSE glass sample after chemical purification treatment. Compared with original chemical composition, the deviation is so small that it can be accepted; thus, we regarded that the purified sample remains the original composition.

Fig. 2 shows the XRD patterns of all Pr^{3+} ions doped glass samples. Even the sample doped with high concentration Pr^{3+} ions as well as 0.4% has no obvious crystallization peaks. In order to make sure of amorphous properties and verify the dispersion of RE ions, the TEM test was further carried out, and the results are shown in Fig. 3 and 4. In both HR-TEM images of GAGSE-0.2 and GAGSE-0.3 samples, no crystal fringe is observed, indicating that the heavily Pr^{3+} ions doped samples still maintain the amorphous state. From the EDS results, it is obvious that all elements are dispersed evenly in the matrix. Comparing the EDS results of GAGSE-0.2 and GAGSE-0.3, it can be seen that the Pr^{3+} gathers a little more densely in some local area when the Pr^{3+}

Tab. 1　The EPMA result of GAGSE-undoped glass after chemical purification treatment

Composition	Theoretical chemical composition/%	Measured composition/%	Error/%
Ge	12	11.23	1.32
As	20.8	20.23	0.83
Ga	4	3.60	2.68
Se	63.2	64.19	0.59
O	0	0.59*	22.3
Si	0	0.16*	26.5
Al	0	0*	100

*The results of these three elements are inauthentic due to the value of error.

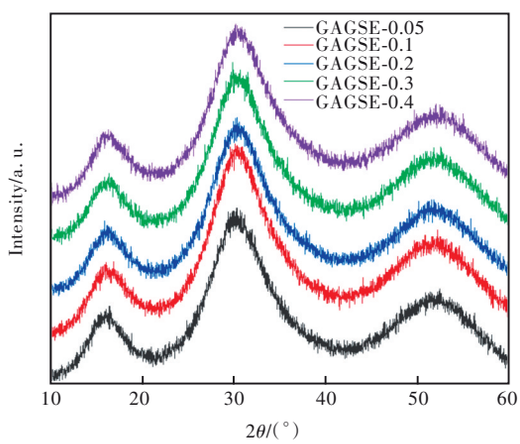

Fig. 2　XRD patterns of 0.05%–0.4% Pr^{3+} ions doped $Ge_{12}As_{20.8}Ga_4Se_{63.2}$ bulk samples

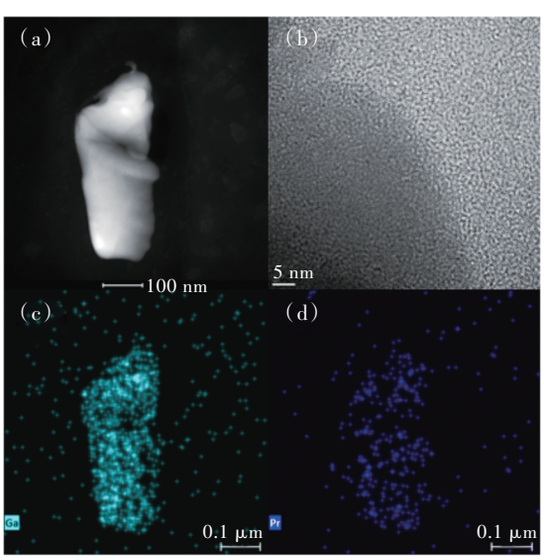

Fig. 3　(a) TEM image of GAGSE-0.2. (b) HR-TEM image of GAGSE-0.2. (c)–(d) The dispersion of Ga, Pr elements in GAGSE-0.2.

ions' concentration increases.

Tab. 2 shows the characteristic temperatures of all Pr^{3+} doped glasses. For the GAGSE-undoped glass, the transition temperature (T_g) is 212 ℃ and the initial crystallization temperature (T_x) is 336 ℃.

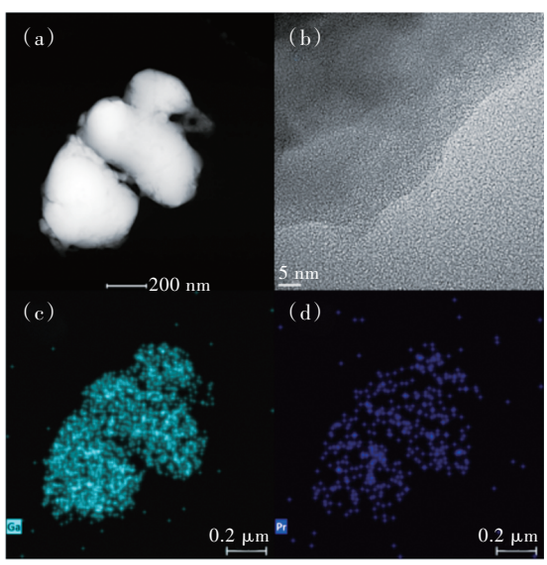

Fig. 4　(a) TEM image of GAGSE-0.3. (b) HR-TEM image of GAGSE-0.3. (c)–(d) The dispersion of Ga, Pr elements in GAGSE-0.3.

Tab. 2　Characteristic temperatures of 0–0.4% Pr^{3+} ions doped $Ge_{12}As_{20.8}Ga_4Se_{63.2}$ glasses

Sample	T_g/℃	T_x/℃	ΔT/℃
GAGSE-undoped	212	336	124
GAGSE-0.1	215	334	119
GAGSE-0.2	217	331	114
GAGSE-0.3	220	330	110
GAGSE-0.4	223	328	105

Parameter of ΔT is used to evaluate the crystallization resistance and vitrification ability of glass. The larger value of ΔT indicates higher glass forming ability and better thermal stability. The ΔT of GAGSE-undoped glass is about 124 ℃, indicating that the $Ge_{12}As_{20.8}Ga_4Se_{63.2}$ glass has great thermal stability as a RE matrix glass. This is beneficial for fiber drawing in the next experiment. When the Pr^{3+} ions are introduced into the matix glass, the T_g is slightly increased whereas T_x is decreased. It is obvious that

the GAGSE-0.4 glass still has a lage ΔT vlaue as well as 105 ℃. Even the content of Pr^{3+} reaches 0.4%, the thermal stability of the glass is still suitable for fiber drawing.

3.2 Absorption and Emission Properties

Fig. 5 shows the absorption spectra of 0.05%–0.4% Pr^{3+} ions doped glasses in the wavelength range of 800–2 500 nm and the electronic energy levels of Pr^{3+} ion. The four obvious absorption bands centered at 1 064, 1 494, 1 608, 2036 nm correspond to the transitions from ground energy level of $^3H_4$ to the excited levels of $^1G_4$, $^3F_4$, $^3F_3$ and $^3F_2$, respectively. The cut-off edge is about 850 nm at the short wavelength because of the band gap absorption. The absorption coefficient of Pr^{3+} ions in $Ge_{12}As_{20.8}Ga_4Se_{63.2}$ glass increases approximately linearly from 0.05% to 0.4% (see Fig. 6), which

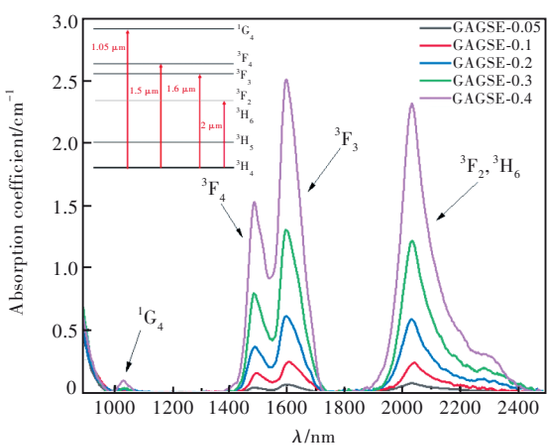

Fig.5 Absorption spectra of 0.05%–0.4% Pr^{3+} ions doped $Ge_{12}As_{20.8}Ga_4Se_{63.2}$ glasses in the range of 850–2 500 nm

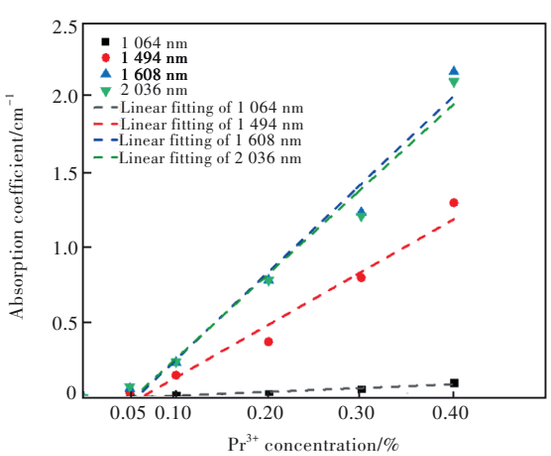

Fig. 6 Linear fitting of absorption coefficient of 0.05%–0.4% Pr^{3+} ions doped $Ge_{12}As_{20.8}Ga_4Se_{63.2}$ glasses at each characteristic absorption peak

confirms the Pr^{3+} ions were dissolved almost homogeneously in the glass.

Based on the absorption spectrum and basic physical parameters, the Judd-Ofelt analysis is used to evaluate the luminescence characteristics[19-20]. The oscillator strengths, Judd-Ofelt intensity parameters Ω_t (t=2, 4, 6) were calculated and summarized in Tab. 3. The values of other reported system glasses are also summarized for comparison. The Ω_t (t=2, 4, 6) are related to the local environment nearby the RE ions. Ω_2 is mainly affected by polarized and asymmetric environment around RE ions, Ω_4 is mainly affected by the acidity and alkaline, and Ω_6 is related to the rigidity of glass[21-23]. In addition, the value of Ω_4/Ω_6 is used to evaluate the spontaneous emission characteristics of RE ions. The two ground state electronic absorption peaks of $^3H_4 \rightarrow {}^3F_4$, $^3F_3$ overlap each other. For J-O analysis, this wide absorption peak can be divided into two characteristic peaks. Taking sample GAGSE-0.4 as an example, the result of division is shown in Fig. 7. The fitting mode is Gaussian-Lorentz and the R^2 is 0.997 455. It can be found that the Ω_t suddenly changed when the concentration of Pr^{3+} ions increased to 0.3%. The sudden increase of Ω_2 implies the asymmetric environment was changed around RE ions. In general, the low symmetry of polyhedral structure and high covalency of constituent bonds will lead to a lager oscillator strength. Compared with the other hosts, Pr^{3+} ions doped GAGSE glass has the lager oscillator strength.

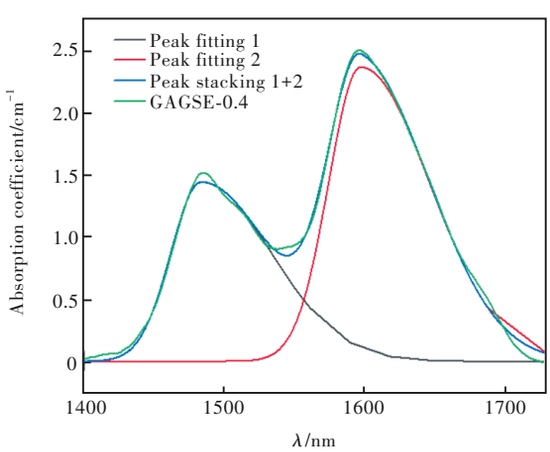

Fig. 7 The division fitting of $^3H_4 \rightarrow {}^3F_4$, $^3F_3$ absorption peak in GAGSE-0.4 glass.

Tab. 3　The J-O intensity parameters and oscillator strength of 0.05%–0.4% Pr^{3+} doped $Ge_{12}As_{20.8}Ga_4Se_{63.2}$ glasses and other hosts[24-28]

Glass	J-O parameters/(10^{-20} cm^2)				Oscillator strength/10^{-6}				Reference
					$^3H_4\rightarrow$				
	Ω_2	Ω_4	Ω_6	Ω_4/Ω_6	$^1G_4$	$^3F_4$	$^3F_3$	$^3F_2$	
GAGSE-0.05	2.37	16.51	8.59	1.92	1.096	13.194	28.857	17.356	
GAGSE-0.1	2.59	14.63	6.05	2.42	1.009	9.712	22.948	15.159	
GAGSE-0.2	2.5	14.15	5.86	2.41	1.074	9.412	22.22	14.663	This work
GAGSE-0.3	2.98	11.37	4.77	2.38	0.812	7.811	18.411	12.965	
GAGSE-0.4	3.3	10.17	4.73	2.15	0.764	7.497	17.136	12.8	
Phosphate	4.26	4.33	6.27	0.69	0.250	10.540	10.640	5.000	[24]
Fluorotellurite	3.57	6.60	5.18	1.27	0.409	4.543	9.668	6.357	[25]
ZBLAN	0.94	6.54	3.84	1.70	3.14	4.05	2.09	0.99	[26]
BKZ	4.92	14.08	8.48	1.66	—	5.49	12.08	7.89	[27]
GAGS	10.4	4.78	10.4	0.46	—	—	—	—	[28]

Fig. 8 shows the infrared transmission spectra of blank and 0.05%–0.4% Pr^{3+} ions doped GAGSE glasses. The infrared cut-off wavelengths are about 18 μm. Because the raw materials have been purified, there are no obvious peaks of impurity absorptions before 9 μm. The strongest absorption peak is at around 4.6 μm which is caused by the absorption of $^3H_5$ energy level of Pr^{3+} ions. However, the absorption of Se—H vibration(3.5 μm and 4.12 μm) with the introduction of RE ions cannot be completely excluded. Besides, the weak absorption peak at 6.3 μm is caused by the impurity absorption of H_2O.

In addition, comparing the Pr^{3+} ions doped and undoped glasses' spectra, it can be found that the Se—H vibration at 3.5 μm and 4.12 μm will appear due to the introduction of Pr^{3+} ions. This is probably because the raw material of Praseodymium powder was generally prepared by a hydrogenation method, which will result in a lot of H elements absorbed in the powder can hard to be totally removed through the subsequent processing process. Moreover, the strong absorption peaks at 9.7 μm and 11.8 μm should be caused by the vibration of As—O and Ge—O, respectively[17]. In fact, it can be seen from the experimental results that the present purified process has an effect on the removal of Se—H, —OH and H_2O, but has no obvious work for the elimination of As—O and Ge—O.

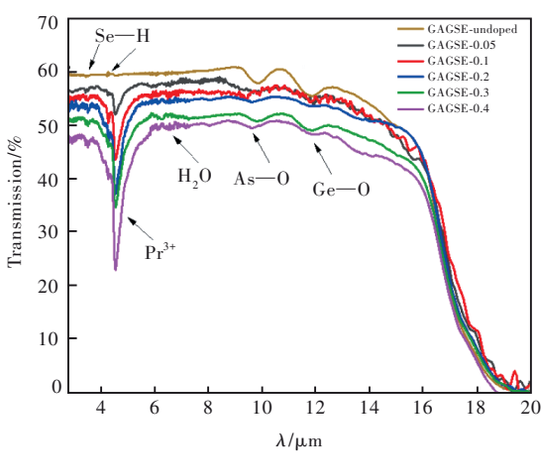

Fig.8　Infrared transmission spectra of 0.05%–0.4% Pr^{3+} ions doped $Ge_{12}As_{20.8}Ga_4Se_{63.2}$ glasses compared with an undoped one in the range of 2–20 μm(The transmission results in this figure are adjusted by multiplying the coefficient for display)

Fig. 9 shows the MIR emission spectra of 0.05%–0.4% Pr^{3+} ions doped $Ge_{12}As_{20.8}Ga_4Se_{63.2}$

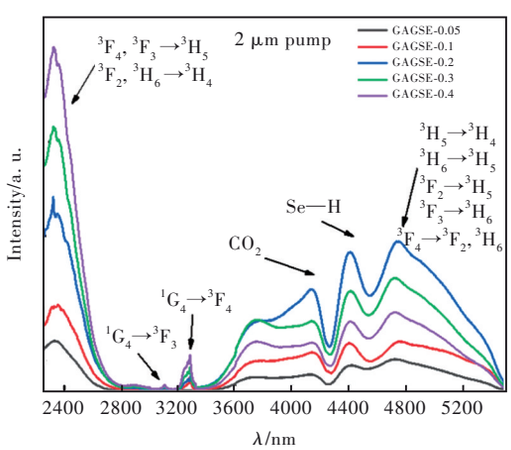

Fig.9　Mid-infrared emission spectra of 0.05%–0.4% Pr^{3+} ions doped $Ge_{12}As_{20.8}Ga_4Se_{63.2}$ glasses pumped by a 2.0 μm laser

glasses ranging from 2 300 nm to 5 500 nm pumped by a 2.0 μm laser. The Pr^{3+} ions have a very wide emission band from 3.4 nm to 5.5 μm. The emission peaks, which centered at 2.33, 3.1, 3.3 μm, correspond to the transitions of $^3F_2/^3H_6 \rightarrow ^3H_4$, $^1G_4 \rightarrow ^3F_3$, and $^1G_4 \rightarrow ^3F_4$, respectively. The electrons that have already been excited to the $^3F_2$ energy level will continue to be excited to the higher $^1G_4$ energy level when pumped by a 2.0 μm laser, as shown in Fig. 10. Actually, the emission peak at 2.33 μm is also contributed by the transition of $^3F_4/^3F_3 \rightarrow ^3H_5$[29]. The broadband luminescence is contributed by the superposition of emission peaks (*i. e.*, $^3F_4 \rightarrow ^3F_2/^3H_6$, $^3F_3 \rightarrow ^3H_6$, $^3F_2 \rightarrow ^3H_5$, $^3H_6 \rightarrow ^3H_5$ and $^3H_5 \rightarrow ^3H_4$). In addition, the dip at 4.24 μm is ascribed to the absorption of CO_2 in the air of the spectrometer and the dip at 4.55 μm is caused by the Se—H bond impurity of the sample itself [8-9,30].

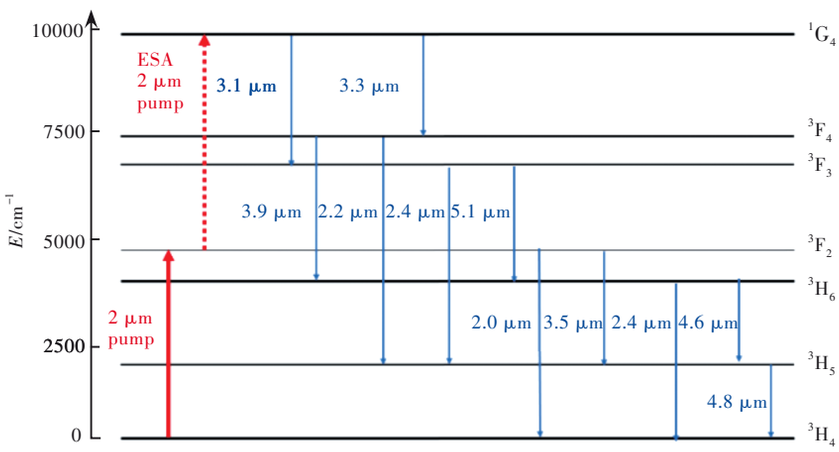

Fig.10 The schematic energy level diagram of Pr^{3+} ions

From the fluorescence spectral variation, it can be seen that when the Pr^{3+} ions' concentration is lower than 0.2%, the fluorescence intensity increases with the increasing of the Pr^{3+} ions' concentration and reaches the maximum at 0.2%. It can also be found that further increasing of Pr^{3+} ions' concentration will enhance the intensities of emissions at 2.33 μm and 3.1 μm but the intensity of wide emission band (3.4–5.5 μm) is decreased. This phenomenon indicates that when the concentration of Pr^{3+} ions is less than or equal 0.2%, most of the Pr^{3+} ions can be evenly distributed in the glass matrix by mainly forming Pr—Se—Ga bonds. However, when the concentration of Pr^{3+} ions is further increased, the finite non-bridging Se can no longer provide enough negative coordination for the Pr^{3+} ions. Therefore, the Pr^{3+} ions gradually begin to be clustered (see Fig. 3(d)) to share ligands by forming of Pr—Se—Pr instead of Pr—Se—Ga ones. In this way, the part of Pr^{3+} ions' clusters contribute little to MIR fluorescence, which ultimately leads to fluorescence quenching[9,30]. Therefore, according to the J-O parameters and fluorescence spectra, it is concluded that the optimal doping concentration of Pr^{3+} ions in this glass matrix is 0.2%. When the concentration is higher than 0.2%, the clusters will bring about fluorescence quenching by depopulating the excited states.

The stimulated emission cross-section of Pr^{3+} in this glass matrix is calculated basing on the Füchtbauer-Ladenburg equation[31]:

$$\sigma_{emi}(\lambda) = \frac{\lambda_p^4 \lambda I(\lambda)}{8\pi c n^2 \tau_{rad} \int \lambda\, I(\lambda)\, d\lambda}, \tag{1}$$

in which the effective line-width, λ_{eff}, of fluorescence band is defined by:

$$\Delta\lambda_{eff} = \frac{\int I(\lambda) d\lambda}{I_{max}}, \tag{2}$$

the $\int I(\lambda) d\lambda$ is the effective peak area and I_{max} is the maximum intensity of each emission peak. λ_p is the center wavelength of emission peak. c is speed of light, n is refractive index, τ_{rad} is the radiation lifetime of transition. The calculated results are listed in Tab. 4. The GAGSE-0.2 glass has a large σ_{emi},

long upper state lifetime, and good branching ratios for transition $^3H_5 \rightarrow {}^3H_4$ and $^3H_6 \rightarrow {}^3H_5$. This is mainly because the chalcogenide glass has a larger refractive index and higher degree of covalent bonding. These characteristics of GAGSE-0.2 glass make it possible for MIR fiber amplifiers and lasers.

Tab. 4　The radiative parameters of 0.05%–0.4% Pr^{3+} doped $Ge_{12}As_{20.8}Ga_4Se_{63.2}$ glasses calculated from J-O parameters

Glass	Transition	λ_{emi}/nm	λ_{eff}/nm	τ_{rad}/ms	β/%	A_{rad}/s^{-1}	$\sigma_{emi}/(10^{-20}\,cm^2)$
GAGSE-0.05	$^1G_4 \rightarrow {}^3F_4$	3 434	131.22	5.92	1.86	133.94	2.491
	$^1G_4 \rightarrow {}^3F_3$	3 000	82.63		0.48	34.88	0.677
	$^3F_3 \rightarrow {}^3H_5$	2 370	—	0.80	15.41	1 243.76	—
	$^3F_4 \rightarrow {}^3H_5$	2 150	—	0.62	35.71	1 592.57	—
	$^3H_5 \rightarrow {}^3H_4$	4 814	752.79	8.59	100	116.36	1.582
	$^3H_6 \rightarrow {}^3H_5$	4 600	734.94	8.16	43.26	122.43	1.401
GAGSE-0.1	$^1G_4 \rightarrow {}^3F_4$	3 434	137.14	8.18	1.68	96.49	1.717
	$^1G_4 \rightarrow {}^3F_3$	3 000	78.80		0.44	25.70	0.523
	$^3F_3 \rightarrow {}^3H_5$	2 370	—	0.89	17.06	1 116.32	—
	$^3F_4 \rightarrow {}^3H_5$	2 150	—	0.77	37.87	1 290.25	—
	$^3H_5 \rightarrow {}^3H_4$	4 814	743.23	10.90	100	91.66	1.305
	$^3H_6 \rightarrow {}^3H_5$	4 600	730.65	10.32	44.16	96.82	1.114
GAGSE-0.2	$^1G_4 \rightarrow {}^3F_4$	3 434	151.73	8.45	1.68	93.43	1.492
	$^1G_4 \rightarrow {}^3F_3$	3 000	102.36		0.45	24.88	0.333
	$^3F_3 \rightarrow {}^3H_5$	2 370	—	0.92	17.04	1 079.16	—
	$^3F_4 \rightarrow {}^3H_5$	2 150	—	0.80	37.86	1 248.55	—
	$^3H_5 \rightarrow {}^3H_4$	4 814	741.76	11.25	100	88.84	1.193
	$^3H_6 \rightarrow {}^3H_5$	4 600	722.42	10.65	44.19	93.83	1.066
GAGSE-0.3	$^1G_4 \rightarrow {}^3F_4$	3 434	171.31	10.04	1.73	79.19	1.120
	$^1G_4 \rightarrow {}^3F_3$	3 000	100.24		0.44	20.43	0.279
	$^3F_3 \rightarrow {}^3H_5$	2 370	—	1.03	18.45	968.83	—
	$^3F_4 \rightarrow {}^3H_5$	2 150	—	0.98	37.50	1 013.12	—
	$^3H_5 \rightarrow {}^3H_4$	4 814	728.76	13.51	100	77.94	1.011
	$^3H_6 \rightarrow {}^3H_5$	4 600	752.17	12.82	44.81	93.83	0.850
GAGSE-0.4	$^1G_4 \rightarrow {}^3F_4$	3 434	163.56	10.04	1.83	79.66	1.180
	$^1G_4 \rightarrow {}^3F_3$	3 000	103.23		0.46	19.98	0.265
	$^3F_3 \rightarrow {}^3H_5$	2 370	—	1.07	18.77	933.02	—
	$^3F_4 \rightarrow {}^3H_5$	2 150	—	1.05	36.39	945.62	—
	$^3H_5 \rightarrow {}^3H_4$	4 814	719.76	14.06	100	71.10	0.984
	$^3H_6 \rightarrow {}^3H_5$	4 600	749.27	13.39	44.85	74.63	0.817

3.3　Fiber Fabrication and Loss

The GAGSE-0.2 glass sample was selected and drawn into a single-mode, double-cladding fiber. Fig. 11 shows the sectional micrographs at different magnifications and the outermost layer is FEP plastic. The diameter of core, inner cladding and outer cladding are 15, 140, 170 μm, respectively. The refractive indexes (n_{core}=2.613, $n_{inner\text{-}cladding}$=2.611, $n_{outer\text{-}cladding}$=2.587) were measured by an IR VASE Mark Ⅱ Spectroscopic Ellipsometer at 2 μm wavelength. The numerical apertures (N. A.) between core and inner cladding is about 0.10, between inner and outer cladding is about 0.35, which were calculated at 2 μm wavelength. There is no obvious crystallization can be found on the surface of fiber, indicating this glass has good ability for fiber fabrication.

The fiber loss of GAGSE-0.2 double-cladding fiber is shown in Fig. 12. The test method is truncation method. The fiber has a lowest loss of 2.95 dB/m at 6.58 μm. The absorption band at 4.6 μm is due to the Pr^{3+} ($^3H_5 \rightarrow {}^3H_4$) and Se—H bonds. The absorption bands at 3.5, 6.3, 7.9 μm should be

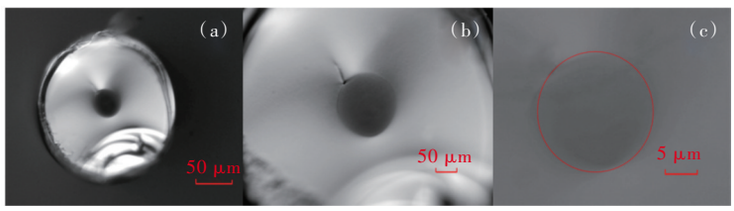

Fig.11 The sectional micrographs of 0.2% Pr^{3+}doped $Ge_{12}As_{20.8}Ga_4Se_{63.2}$ double-cladding fiber. (a)50× magnified image of whole fiber. (b)100× magnified image of outer cladding and inner cladding. (c)500× magnified image of core and inner cladding.

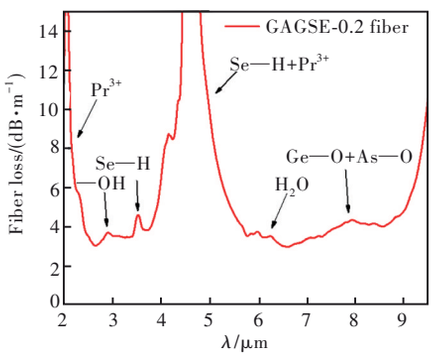

Fig.12 The optical loss of 0.2% Pr^{3+}doped $Ge_{12}As_{20.8}Ga_4Se_{63.2}$ double-cladding fiber

—OH, Se—H, H_2O and oxide impurities(Ge—O, As—O), respectively.

4 Conclusion

The new glass composition in the Ge-As-Ga-Se chalcogenide system, *i. e.* $Ge_{12}As_{20.8}Ga_4Se_{63.2}$ shows high Pr^{3+} ions' solubility(0.4% in weight at maximum) and good thermal characteristic ($T_x-T_g\geqslant105$ ℃). The Pr^{3+} ions have a very wide emission band from 3.4 μm to 5.5 μm and the 0.2%(in weight) Pr^{3+} ions doped glass shows the best mid-infrared emission characteristic. Through physical and chemical purification, the impurity content can be effectively reduced to an acceptable level. The 0.2% (in weight) Pr^{3+} ions doped $Ge_{12}As_{20.8}Ga_4Se_{63.2}$ glass was successfully drawn into a step-index, double-cladding fiber by a multistage rod-in-tube method, and the lowest loss is 2.95 dB/m at 6.58 μm. To sum up, it should be a good potential gain medium to realize mid-infrared fiber lasers working at 3.5-5.5 μm.

Response Letter is available for this paper at: http://cjl.lightpublishing.cn/thesisDetails#10.37188/CJL.20220088.

References:

[1] WILLER U, SARAJI M, KHORSANDI A, *et al*. Near- and mid-infrared laser monitoring of industrial processes, environment and security applications [J]. *Opt. Lasers Eng.*, 2006, 44(7): 699-710.

[2] SEDDON A B. Chalcogenide glasses: a review of their preparation, properties and applications [J]. J. *Non-Cryst. Solids*, 1995, 184: 44-50.

[3] HEO J, SANGHERA J S, MACKENZIE J D. Chalcohalide glasses for infrared fiber optics [J]. *Opt. Eng.*, 1991, 30(4): 470-479.

[4] WAYNANT R W, ILEV I K, GANNOT I. Mid-infrared laser applications in medicine and biology [J]. *Philos. Trans. Roy. Soc. A-Math. Phys. Eng. Sci.*, 2001, 359(1780): 635-644.

[5] UEMURA O, HAYASAKA N, TOKAIRIN S, *et al*. Local atomic arrangement in Ge-Te and Ge-S-Te glasses [J]. J. *Non-Cryst. Solids*, 1996, 205-207: 189-193.

[6] SCHNEIDER J. Fluoride fibre laser operating at 3.9 μm [J]. *Electron. Lett.*, 1995, 31(15): 1250-1251.

[7] SCHNEIDE J, CARBONNIER C, UNRAU U B. Characterization of a Ho^{3+}-doped fluoride fiber laser with a 3.9-μm emission wavelength [J]. *Appl. Opt.*, 1997, 36(33): 8595-8600.

[8] TANG Z Q, FURNISS D, FAY M, *et al*. Mid-infrared photoluminescence in small-core fiber of praseodymium-ion doped selenide-based chalcogenide glass [J]. *Opt. Mater. Express*, 2015, 5(4): 870-886.

[9] LIU Z J, BIAN J Y, HUANG Y, *et al*. Fabrication and characterization of mid-infrared emission of Pr^{3+} doped selenide chalcogenide glasses and fibres [J]. *RSC Adv.*, 2017, 7(66): 41520-41526.

[10] SOJKA L, TANG Z Q, FURNISS D, *et al*. Mid-infrared emission in Tb^{3+}-doped selenide glass fiber [J]. *J. Opt. Soc. Amer.*

B, 2017,34(3):A70-A79.

[11] CUI J, XIAO X S, XU Y T, *et al.* Mid-infrared emissions of Dy^{3+} doped Ga-As-S chalcogenide glasses and fibers and their potential for a 4.2 μm fiber laser [J]. *Opt. Mater. Express*, 2018,8(8):2089-2102.

[12] SÓJKA Ł, TANG Z Q, ZHU H, *et al.* Study of mid-infrared laser action in chalcogenide rare earth doped glass with Dy^{3+}, Pr^{3+} and Tb^{3+} [J]. *Opt. Mater. Express*, 2012,2(11):1632-1640.

[13] AITKEN B G, PONADER C W, QUIMBY R S. Clustering of rare earths in GeAs sulfide glass [J]. *C. R. Chim.*, 2002,5(12):865-872.

[14] NUNES J J, SÓJKA Ł, CRANE R W, *et al.* Room temperature mid-infrared fiber lasing beyond 5 μm in chalcogenide glass small-core step index fiber [J]. *Opt. Lett.*, 2021,46(15):3504-3507.

[15] HU R F, HAN J H, FENG G Y, *et al.* Study on the phase transition of fracture region of laser induced damage in fused glass by focused nanosecond pulse [J]. *Optik*, 2017,140:427-433.

[16] ZHU L, YANG D D, WANG L L, *et al.* Optical and thermal stability of Ge-As-Se chalcogenide glasses for femtosecond laser writing [J]. *Opt. Mater.*, 2018,85:220-225.

[17] SHIRYAEV V S, VELMUZHOV A P, TANG Z Q, *et al.* Preparation of high purity glasses in the Ga-Ge-As-Se system [J]. *Opt. Mater.*, 2014,37:18-23.

[18] SHIRYAEV V S, KARAKSINA E V, CHURBANOV M F, *et al.* Special pure germanium-rich Ga-Ge-As-Se glasses for active mid-IR fiber optics [J]. *Mater. Res. Bull.*, 2018,107:430-437.

[19] JUDD B R. Optical absorption intensities of rare-earth ions [J]. *Phys. Rev.*, 1962,127(3):750-761.

[20] OFELT G S. Intensities of crystal spectra of rare-earth ions [J]. *J. Chem. Phys.*, 1962,37(3):511-520.

[21] TANABE S, OHYAGI T, SOGA N, *et al.* Compositional dependence of Judd-Ofelt parameters of Er^{3+} ions in alkali-metal borate glasses [J]. *Phys. Rev.* B *Condens. Matter*, 1992,46(6):3305-3310.

[22] GUO Q, XU Y T, GUO H T, *et al.* Effect of iodine(I_2) on structural, thermal and optical properties of Ge-Sb-S chalcohalide host glasses and ones doped with Dy [J]. J. *Non-Cryst. Solids*, 2017,464:81-88.

[23] WANG Z X, GUO H T, XIAO X S, *et al.* Synthesis and spectroscopy of high concentration dysprosium doped GeS_2-Ga_2S_3-CdI_2 chalcohalide glasses and fiber fabrication [J]. *J. Alloys Compd.*, 2017,692:1010-1017.

[24] CZAJA M, BODYŁ S, GABRYŚ-PISARSKA J, *et al.* Applications of Judd-Ofelt theory to praseodymium and samarium ions in phosphate glass [J]. *Opt. Mater.*, 2009,31(12):1898-1901.

[25] ZHOU B, TAO L L, TSANG Y H, *et al.* Superbroadband near-IR photoluminescence from Pr^{3+}-doped fluorotellurite glasses [J]. *Opt. Express*, 2012,20(4):3803-3813.

[26] BINNEMANS K, VERBOVEN D, GÖRLLER-WALRAND C, *et al.* Absorption and magnetic circular dichroism spectra of praseodymium doped fluorozirconate(ZBLAN) glass [J]. *J. Alloys Compd.*, 1997,250(1-2):321-325.

[27] SUBRAMANYAM Y, MOORTHY L R, LAKSHMAN S V J. Spectroscopic investigations of the Pr(Ⅲ) ion in certain ternary sulfate glasses [J]. J. *Less-Common Metals*, 1989,148(1-2):363-368.

[28] QUIMBY R S, AITKEN B G. Effect of population bottlenecking in Pr fiber amplifiers with low-phonon hosts [J]. *IEEE Photonics Technol. Lett.*, 1999,11(3):313-315.

[29] SUJECKI S, SOJKA L, BERES-PAWLIK E, *et al.* Experimental and numerical investigation to rationalize both near-infrared and mid-infrared spontaneous emission in Pr^{3+} doped selenide-chalcogenide fiber [J]. *J. Lumin.*, 2019,209:14-20.

[30] SAKR H, TANG Z, FURNISS D, et al. Towards mid-infrared fiber-lasers: rare earth ion doped, indium-containing, selenide bulk glasses and fiber [C]. *Proceedings Volume* 8938, *Optical Fibers and Sensors for Medical Diagnostics and Treatment Applications* XIV, *San Francisco, California, United States*, 2014.

[31] FAN T Y, KOKTA M R. End-pumped Nd:LaF_3 and Nd:$LaMgAl_{11}O_{19}$ lasers [J]. *IEEE J. Quantum Electron.*, 1989,25(8):1845-1849.

许晨煜(1998-),男,陕西咸阳人,硕士研究生,2019年于四川大学获得学士学位,主要从事稀土掺杂硫系玻璃光纤材料的研究。

E-mail:xuchenyu@opt.cn

郭海涛(1980-),男,湖北襄阳人,博士,研究员,博士生导师,2007年于武汉理工大学获得博士学位,主要从事特种玻璃光纤和光纤器件方面的研究。

E-mail:guoht_001@opt.ac.cn